

# Highly Thermal Conductive Copper Nanowire Composites with Ultralow Loading: Toward Applications as Thermal Interface Materials

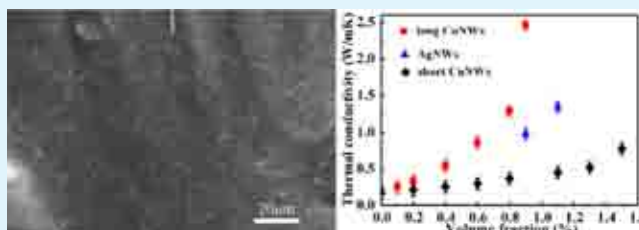
Shouling Wang, Yin Cheng, Ranran Wang,\* Jing Sun,\* and Lian Gao

The State Key Lab of High Performance Ceramics and Superfine Microstructure, Shanghai Institute of Ceramics, Chinese Academy of Science, 1295 Dingxi Road, Shanghai 200050, P. R. China

## S Supporting Information

**ABSTRACT:** Thermal interface materials (TIMs) are of ever-rising importance with the development of modern microelectronic devices. However, traditional TIMs exhibit low thermal conductivity even at high loading fractions. The use of high-aspect-ratio material is beneficial to achieve low percolation threshold for nanocomposites. In this work, single crystalline copper nanowires with large aspect ratio were used as filling materials for the first time. A thermal conductivity of 2.46 W/mK was obtained at an ultralow loading fraction,  $\sim 0.9$  vol %, which was enhanced by 1350% compared with plain matrix. Such an excellent performance makes copper nanowires attractive fillers for high-performance TIMs.

**KEYWORDS:** copper nanowires, growth, composites, thermal interface materials, thermal conductivity, percolation



## 1. INTRODUCTION

Inefficient heat dissipation is the limiting factor for the performance and reliability of microelectronics.<sup>1</sup> This problem has become much more severe with the increasing power densities in many modern microelectronic devices.<sup>2</sup> Efficient heat transfer from an integrated circuit (IC) to a heat sink is a critical issue for the progress of modern electronic devices.<sup>3</sup> Unfortunately, microscopic roughness of the IC and heat sink surfaces results in asperities between the two mating surfaces, which prevent ideal thermal contact.<sup>4</sup> Therefore, thermal interface materials (TIMs) with high thermal conductivity and good conformability are generally applied between the two mating surfaces to provide a good heat conduction path.<sup>5</sup>

TIMs are typically made of low modulus polymer matrix filled with high thermally conductive particles (typical size about 2–25  $\mu\text{m}$ ).<sup>6</sup> Ceramic (BN, AlN, etc.), metal (silver, copper, nickel, aluminum, etc.) and metal oxide particles ( $\text{Al}_2\text{O}_3$ , MgO, etc.) are typically used as fillers for conventional TIMs.<sup>7–12</sup> However, high loading fractions are required to achieve thermal conductivity in the range of  $\sim 1$ –5 W/mK.<sup>6</sup> The limited thermal conductivity as well as the high cost hardly meet the increasing thermal dissipation demand for modern industry. Carbon nanotubes and graphene have been widely studied as filling materials on the basis of their high intrinsic thermal conductivity,<sup>13–15</sup> which ranges from 3000 to 6000 W/mK.<sup>3,4,16</sup> However, the reported thermal conductivity of composites based on them is rather unsatisfying on account of their intrinsic defects and high thermal contact resistance.<sup>17–19</sup>

Except for the thermal conductivity of filling materials, morphology also plays an important role in the performance of TIMs.<sup>20</sup> Compared with microfillers, improvements on both thermal and mechanical properties have been demonstrated for nanofillers.<sup>21</sup> Varieties of nanostructures have been successfully synthesized, such as nanoparticles, nanorods, nanocubes, nanocages, nanowires, etc.<sup>22</sup> Among them, nanowires are preferable for TIMs since their inherent continuity as well as the large aspect ratio would lead to lower percolation threshold.<sup>23</sup> Recently, silver nanowires (AgNWs) have been extensively studied as filling materials for TIMs because of their high thermal conductivity and mature fabrication process.<sup>24</sup> Composites based on AgNWs exhibited superior thermal conducting performance.<sup>25</sup> However, high cost is a major bottleneck for their industrial application. Compared with silver, copper is an earth abundant element and 100 times less expensive, and most importantly, copper also has a high thermal conductivity, 400 W/mK for bulk copper.<sup>26</sup> This makes copper nanomaterials more competitive as TIMs' fillers. However, to the best of our knowledge, TIMs based on CuNWs were seldom reported, which mainly attributes to the immature fabrication method of CuNWs.

A number of fabrication methods for CuNWs have been developed, such as electrospinning,<sup>27</sup> electrochemical deposition,<sup>28</sup> template or membrane method,<sup>29</sup> and reverse micelle system.<sup>30</sup> However, the above methods are generally not

Received: January 2, 2014

Accepted: April 9, 2014

Published: April 9, 2014

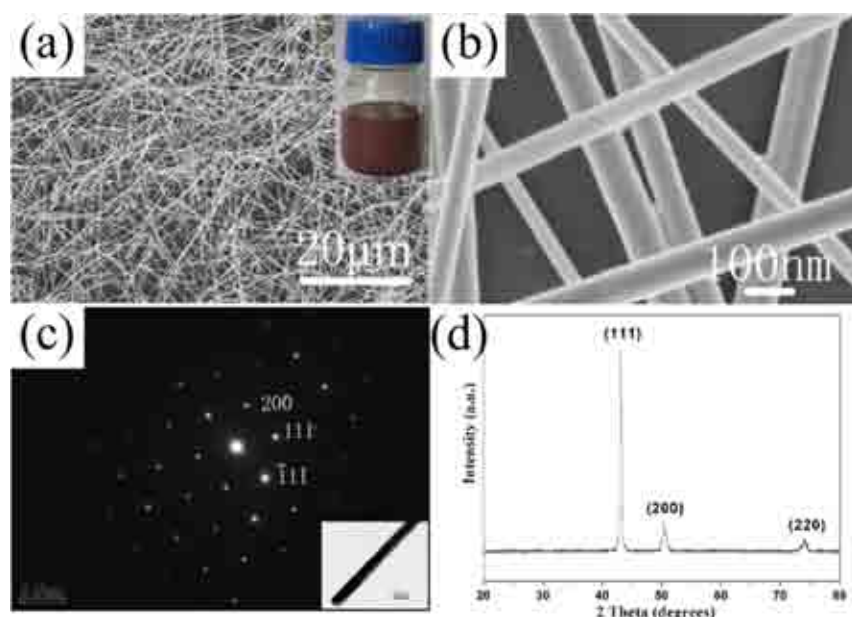


**Figure 1.** (a, b) SEM images of CuNWs prepared. (c) SAED pattern of CuNWs in this work. (d) XRD pattern of CuNWs.

applicable because of the limitation in mass production and process complexity.<sup>31</sup> The newly developed chemical reduction method in aqueous solution has drawn much attention since it is facile and with low cost.<sup>32,33</sup> This technique mainly relies on the reduction of  $\text{Cu}^{\text{II}}$  to  $\text{Cu}^0$  in an aqueous solution with the help of reducing agent (such as glucose or hydrazine) and capping agent (like cetyltrimethylammonium bromide). However, the procedure often produces nanowires with bad dispersion and easily to be oxidized.<sup>34</sup> Our group has proposed a nonaqueous synthesis of ultralong single-crystalline CuNWs recently.<sup>35</sup> This procedure mainly relies on the self-catalytic growth of CuNWs within a liquid-crystalline medium with the presence of platinized silicon wafers. However, the big challenge for this method is its low yield and instability when the production was scaled up.

In this work, a large-scale synthesis procedure for CuNWs was developed on the basis of our previous fabrication method. Well dispersed single-crystalline CuNWs with large aspect ratio were successfully synthesized through the modified fabrication procedure. The yield was increased by 32 times and could be applied as building blocks for TIMs. CuNW–polymer composites with different filling fractions were fabricated and the thermal conductivity was characterized systematically. Acrylate was chosen as matrix material since it could be easily cured under ultraviolet (UV) irradiation, which avoided the sedimentation of fillers. With the loading fraction of CuNWs as 0.9 vol %, the thermal conductivity of composites was 2.46 W/mK, increased by 1350% compared with the pristine polymer matrix. This is higher than that of composites filled with commercial AgNWs at 1.1 vol % and outperforms carbon and metallic nanomaterial based thermal conductive composites. To the best of our knowledge, this is the first time to use ultralong CuNWs as thermal conductive fillers and achieve the high thermal conductivity at such low loading percentage.

## 2. EXPERIMENTAL SECTION

**Preparation of CuNWs.** In a typical synthesis, 5 g of cetyltrimethylammonium bromide (CTAB) and 80 g of hexadecylamine (HDA) were melted at 180 °C first. Then 2 g of copper acetylacetonate and 5  $\mu\text{L}$  of platinum nanoparticles dispersed in

ethylene glycol was added to the above melt one after another. Platinum nanoparticles were produced according to the literature report.<sup>36</sup> The mixture was then heated to 180 °C and kept for 10 h. After the reaction, the resulting reddish brown products were washed with toluene thoroughly to remove the residual organics and the resulting cottonlike products were then kept in ethanol in a sealed container at room temperature.

### Preparation of Metal Nanowire–Polyacrylate Composites.

CuNW–polyacrylate composites were prepared by solution mix processing. Typically, the liquid monomer of acrylate (SR601) was first fully mixed with photo initiator. The stored CuNWs were sonicated for 1 min first, then added into the above liquid mixture, and then stirred for 10 min. After that, the suspension was left in a vacuum drying oven until the solvent was fully evaporated. The content of CuNWs was calculated by the weight increase after solvent evaporation. Finally, the uncured composites mixtures were drop cast into self-made molds by doctor blading. Samples with thickness about 500  $\mu\text{m}$  were fabricated under UV irradiation for 5 min. For comparison, composites filled with commercial AgNWs and short CuNWs were also prepared following the same procedure.

**Characterization.** Morphologies of CuNWs and metal nanowires–polymer composites were characterized by field-emission scanning electron microscopy (FE-SEM, JSM-6700F) Transmission electron microscope (TEM) was conducted on a JEM-2100F. Composites were frozen by liquid nitrogen to break into small pieces for SEM analysis. X-ray diffraction (XRD) was carried out on a D/max 2550 V X-ray diffraction-meter with  $\text{Cu-K}\alpha$  irradiation at  $\lambda = 1.5406 \text{ \AA}$ . Thermal conductivity of the composites was measured using the laser flash method and determined from the equation  $\kappa = \alpha\rho C_p$ , where  $\alpha$  is the thermal diffusivity value,  $\rho$  is density, and  $C_p$  is the specific heat capacity of composites. Density ( $\rho$ ) was obtained using the equation  $\rho = m/(\pi r^2 d)$ , where  $m$  is the mass of the composite sample and  $d$  and  $r$  are the thickness and the radius of the sample, respectively. The mass was measured on MS105 Semi-Micro Balance with the system error of 0.0001  $\text{g cm}^{-3}$ . Thermal diffusivity measurement was carried out with NETZSCH LZF 207 based on GJB1201.1–91. After calibration, the system error is within 5%. Specific heat capacity was measured by differential scanning calorimetry (PE DSC-2C) in nitrogen, with sapphire as reference sample. The temperature ranged from room temperature to 90 °C at a heating rate of 10 °C/min. Its system error is about 5–6%. The relative error is between 6 and 24%, depending on the samples. The relative error of the conductivity was calculated by the method illustrated in Yu's work.<sup>37</sup> The electrical resistivity was

measured using a four-point-probe measurement system (ACCENT HL5500) with silver paste as the contact pad.

### 3. RESULTS AND DISCUSSION

In our previous work, a nonaqueous procedure was proposed to synthesize ultralong CuNWs with good dispersibility. Unfortunately, only  $\sim 5$  mg of CuNWs could be obtained at one time, which was far below the demands of real applications. Besides, platinum sputtered on silicon wafers were used as catalysts, which makes it difficult for precise control, therefore leading to the instability of the synthesis. In this work, with platinum nanoparticles as catalyst, 160 mg of CuNWs could be obtained at one time. Large amount of ultralong CuNWs entangled together and settled down to the bottom of the glass vessel, which makes the collection of CuNWs very easy (see Figure S1 in the Supporting Information).

Images a and b in Figure 1 show the SEM images of the CuNWs. The average diameter of the CuNWs was about 80 nm, and the length varied from several tens to hundreds of micrometer. The aspect ratio was as high as  $1 \times 10^2$  to  $1 \times 10^3$ . This was in good accordance with the earlier report.<sup>35</sup> Besides, the nanowires were found to be highly flexible as some of them showed bending more than  $180^\circ$  without any fracture. We also found that the above ultralong CuNWs could break into short ones ( $<20 \mu\text{m}$ ) through sonication (shown in Figure S2 in the Supporting Information). Figure 1c is the selected area electron diffraction (SAED) pattern of the nanowires. This pattern shows that the nanowires are single-crystalline growing along the [011] direction. Figure 1d shows an XRD pattern of copper nanowires. The three peaks at  $2\theta = 43.5$ ,  $50.8$ , and  $74.1^\circ$  correspond to diffractions from {111}, {200}, and {220} planes of face-centered cubic Copper (JCPDS # 03-1018), respectively. No diffraction peaks of CuO and Cu<sub>2</sub>O were observed, indicating that the CuNWs were under good preservation.

CuNWs are expected to be ideal filling materials for TIMs considering their high intrinsic thermal conductivity, large aspect ratio and low cost. CuNWs-polyacrylate composites at different volume fractions were fabricated and their thermal conductivity was measured systematically. Polyacrylate was chosen as resin matrix since it can be polymerized in several minutes by UV irradiation, which would avoid the aggregation and sedimentation of nanowires in polymerization process with long time. Figure 2 is SEM images of the cross sections of long-CuNWs-polyacrylate composites, which discloses the homogeneous dispersion of CuNWs in the polymer matrix. The added amount of CuNWs ranged from 0.1 to 0.9 vol %. When the loading percentage of CuNWs was increased to 0.9 vol %, a continuous nanowire network formed, as clearly shown in Figure 2f. In order to verify the superiority of long CuNWs prepared in this work, short CuNWs and commercial AgNWs (average length,  $\sim 20 \mu\text{m}$ ; average diameter,  $\sim 120$  nm) were also used as filling materials to make composites following the same fabrication procedure. The short CuNWs were obtained by cutting long nanowires through sonication. After sonication, centrifugation was conducted to remove long nanowires, leaving nanowires shorter than  $20 \mu\text{m}$  in the supernatant. Figure 3 are SEM images of the cross-sections of short-CuNW-polyacrylate composites. Unlike polyacrylate filled with long CuNWs, continuous network barely formed in the short-CuNW-polyacrylate composites, even when the volume fraction was further increased to 1.5 vol %. Similar phenomenon was observed in AgNWs-polyacrylate composites,

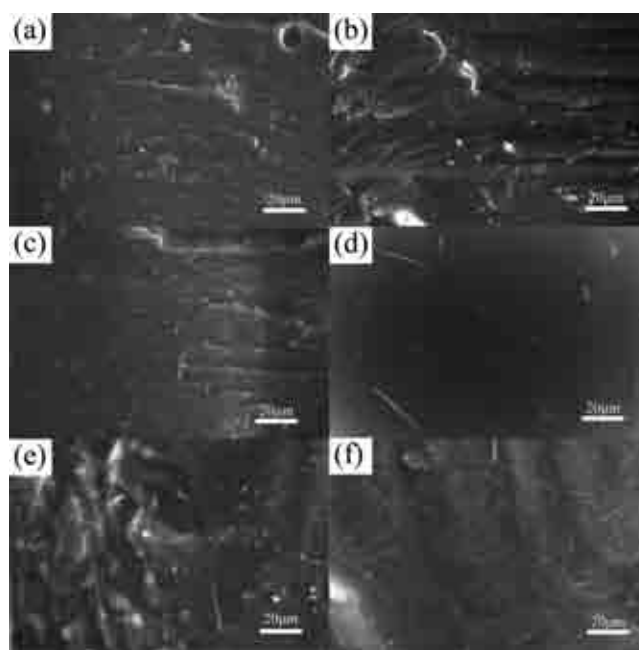


**Figure 2.** SEM images of long-CuNW-polyacrylate composites: (a) 0.1, (b) 0.2, (c) 0.4, (d) 0.6, (e) 0.8, and (f) 0.9 vol %.

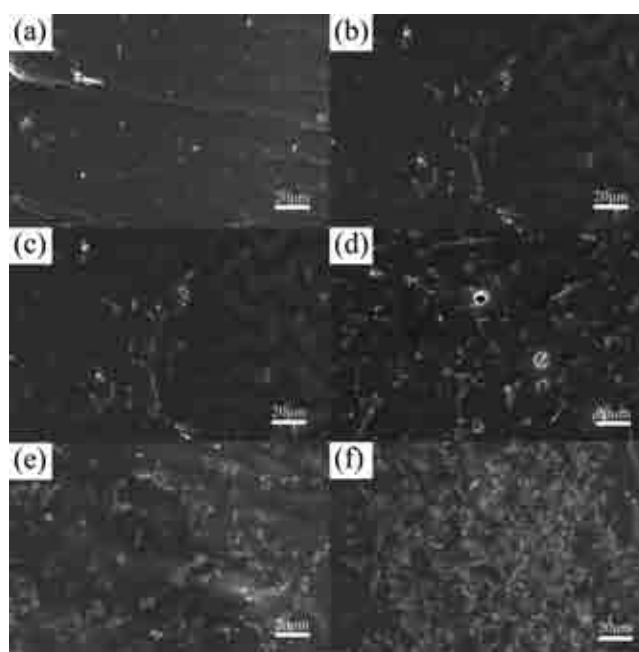


**Figure 3.** SEM images of short-CuNW-polyacrylate composites: (a) 0.4, (b) 0.6, (c) 0.8, (d) 1.1, (e) 1.3, and (f) 1.5 vol %.

as seen in Figure S3 in the Supporting Information. The SEM analysis is in accordance with percolation threshold theory, the main concept of which is fillers with large aspect ratio connected at lower loading fraction. On the basis of the above analysis, polyacrylate filled with long CuNWs should have higher thermal conductivity compared with that filled with short CuNWs and commercial AgNWs at the same loading fraction, which will be discussed in detail in the following part.

Figure 4a shows the thermal conductivity of the three composites at room temperature with a series of volume fraction of nanowires. Enhancement on thermal conductivity has been found for all measured composites. The measured



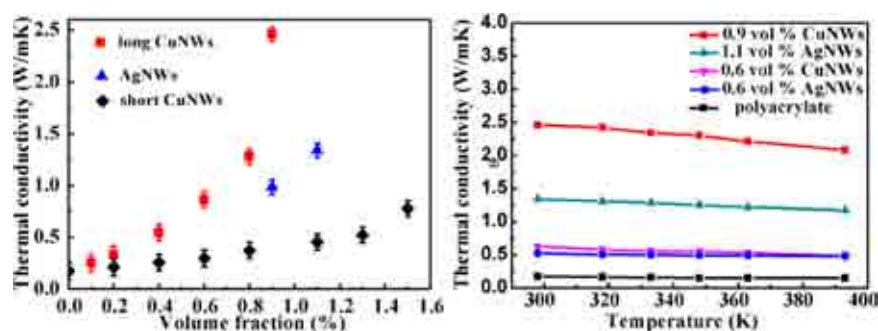


**Figure 4.** (a) Experimental thermal conductivity of metal nanowire–polyacrylate composites with different volume fractions at 298 K; (b) thermal conductivity of metal nanowire–polyacrylate composites as a function of temperature.

thermal conductivity of polyacrylate ester was 0.17 W/mK, which is consistent with the acrylate vendor's specification. For composites loaded with 1.5 vol % short CuNWs, the thermal conductivity was 0.77 W/mK, which is enhanced by 350% compared to the pristine polyacrylate matrix.

A lower percolation threshold and higher thermal conductivity has been achieved for composites filled with long CuNWs. According to the percolation threshold theory,<sup>38</sup> at a low loading fraction, both the electronic thermal conduction and phonon thermal conduction are hindered, since the fillers rarely form a connected network for heat flow in the matrix material. When the filling fraction reaches a critical value, the percolation threshold, a dramatic increase of thermal conductivity will occur. At this situation, filling materials contact each other, forming a good thermally conductive network in the resin. For composites filled with short CuNWs, the thermal conductivity increased slightly with the increase of loading fraction, and no magnificent change was observed even when the loading fraction increased to 1.5 vol %. In this case, the percolation threshold was not achieved, which is consistent with the SEM analysis. In the case of composites filled with long CuNWs, analogous variation trend on thermal conductivity was found below the loading fraction of 0.8 vol %. Nevertheless, their thermal conductivity was much higher than that of composites filled with short CuNWs under the same loading fraction, and it increased much faster as the loading fraction increases. Moreover, a sharp increase on thermal conductivity was observed when the loading fraction increased from 0.8 vol % to 0.9 vol %. It is believed that the percolation threshold was achieved at ~0.9 vol % and continuous CuNWs network was formed. The thermal conductivity reached the value of 2.46 W/mK, corresponding to the enhancement of ~1350%. For comparison, AgNW–polyacrylate composites with the same procedure were prepared considering the better thermal conductivity of silver. However, the measured thermal conductivity value was 1.4 W/mK at 1.1 vol %, lower than that of long-CuNWs-polyacrylate composite at 0.9 vol %, unexpectedly. This may owe to the larger aspect ratio of CuNWs which contributes to the high performance. It is even higher than that of composites filled with commercial AgNWs at the same volume fraction, which is beyond our expectation since silver has higher thermal conductivity. This can be explained by the well-connected conducting network formed with long CuNWs. Yu's work also indicated that fully connected conducting path will lead to high thermal conductivity even at low loading percentage.<sup>39</sup> The thermal conductivity of the long-CuNW–polyacrylate composite is

extremely high compared to previous reports, as listed in Table 1, especially at such low loading fraction.

**Table 1. Thermal Conductivity Enhancement in TIM Composites**

filler	fraction	$\kappa$ enhancement (%)	method	reference
graphene	10 vol %	2300	laser flash	40
graphite	20 wt %	1800	laser flash	41
SWCNT	1 vol %	180	steady state	42
MWCNT	3.8 wt %	65	ASTM	43
BN	30 vol %	2300	laser flash	44
AlN	10 wt %	118	steady state	45
CuNWs	0.9 vol %	1350	laser flash	This work
AgNWs	1.1 vol %	680	laser flash	This work

The influence of temperature on thermal conductivity was investigated as shown in Figure 4b. The thermal conductivity of CuNWs-polyacrylate composites decreases with increasing temperature, while that of pristine polyacrylate ester was nearly independent of temperature. This suggests the thermal conduction was mainly attributed to the linked CuNWs in composites. For metal materials, heat is mainly carried by electrons. When temperature was elevated, the scattering of electrons would be enhanced, which resulted in the decrease in thermal conductance. This phenomenon has also been observed in other composites.<sup>40</sup>

To better demonstrate the superiority of long CuNWs, the thermal conduction model of metal nanowire–polyacrylate composites was proposed, as illustrated in Figure 5. Polymer



**Figure 5.** Illustration of thermally conductive paths for composites filled with (a) long CuNWs, (b) AgNWs, and (c) short CuNWs.

usually has a low thermal conduction because no effective thermally conductive networks could be formed because of the strong phonon scattering of the randomly entangled molecule chains.<sup>46</sup> The introduced thermally conductive particles could help to improve the thermal conduction, however, the outcomes were not always desirable owing to the adjunctive thermal resistance. The extra thermal resistance in composites was mainly originated from three parts, (1) contact resistance between metal nanowires,  $R_{c1}$ ; (2) contact resistance between

metal nanowires and matrix materials,  $R_{c2}$ ; and (3) the intrinsic resistance of metal nanowires named as  $R_b$ .<sup>47</sup> Contacting resistance can be expressed as  $R_c = \rho_c/d$ , where  $\rho_c$  is the contacting resistivity and  $d$  is the diameter of the contacting area.<sup>38</sup> It is clear that higher loading fraction is needed to form the thermally conductive network for composites filled with small aspect ratio fillers. Thus, the higher contact resistance  $R_c$  was generated because of the relatively greater number of contact points and a small contact area, which led to lower thermal conductivity of the composites.

The electrical conductivity of the composites was also tested to demonstrate the continuity of long CuNWs in the composites. At a filling fraction of 0.6 vol %, the conductivity was about  $1 \times 10^{-6}$  S/cm for both long CuNWs and short CuNW-based composites, as seen from Figure 6. With the

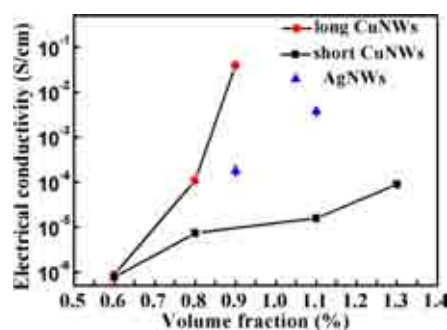


**Figure 6.** Electrical conductivity of the metal nanowire–polyacrylate composites with different loading percentage.

increase in loading percentage, the conductivity of all the three metal nanowire composites increased apparently, among which, that of the long CuNWs composites increased the most rapidly, testifying the superiority of the long CuNWs on forming conductive network. At the filling fraction of 0.9 vol %, the conductivity of long-CuNW composite reaches 0.04 S/cm, which is 10 times larger than that of Ag NW composites with the filling fraction of 1.1 vol %. The variation trend of the electron conductivity is consistent with that of the thermal conductivity, indicating the dominant contribution of electron transport to the thermal conduction in these composite materials.

#### 4. CONCLUSIONS

In this work, single-crystalline CuNWs with large aspect ratio and high yield were successfully synthesized. CuNW–polyacrylate composites with different loading percentage were prepared and their thermal conductivity values were measured by laser flash method. The thermal conductivity value of long-CuNW–polyacrylate is 2.46 W/mK at a filler volume fraction 0.9 vol %, enhanced by 1350% compared with plain matrix. This is higher than that of composites filled with commercial AgNWs at 1.1 vol % and outperforms carbon and metallic nanomaterial based thermal conductive composites. The large aspect ratio and single-crystalline structure are responsible for the high thermal conductivity at such low loading percentage. Such excellent performance makes long CuNWs attractive fillers for TIMs.

#### ■ ASSOCIATED CONTENT

##### Supporting Information

Supplementary photograph of the resulting long CuNWs, SEM figures of short CuNWs, and cross-sectional SEM images of AgNW–polyacrylate composites. This material is free of charge via the Internet at <http://pubs.acs.org>.

#### ■ AUTHOR INFORMATION

##### Corresponding Authors

\*E-mail: wangranran@mail.sic.ac.cn. Tel.: +86-21-52414301.

Fax: +86-21-52413122.

\*E-mail: jingsun@mail.sic.ac.cn

##### Notes

The authors declare no competing financial interest.

#### ■ ACKNOWLEDGMENTS

This work was financially supported by National Natural Science Foundation of China (Grant 61301036), Shanghai Municipal Natural Science Foundation (Grant 13ZR1463600), and support from Innovation Projects of Shanghai Institute of Ceramics.

#### ■ REFERENCES

- (1) Lin, W.; Moon, K. S.; Wong, C. P. A Combined Process of In Situ Functionalization and Microwave Treatment to Achieve Ultra-small Thermal Expansion of Aligned Carbon Nanotube-Polymer Nanocomposites: Toward Applications as Thermal Interface Materials. *Adv. Mater.* **2009**, *21*, 2421–2424.
- (2) Tan, F. L.; Tso, C. P. Cooling of Mobile Electronic Devices Using Phase Change Materials. *Appl. Therm. Eng.* **2004**, *24*, 159–169.
- (3) Prasher, R. Thermal Boundary Resistance and Thermal Conductivity of Multiwalled Carbon Nanotubes. *Phys. Rev. B* **2008**, *77*, 075424.
- (4) Shahil, K. M. F.; Balandin, A. A. Thermal Properties of Graphene and Multilayer Graphene: Applications in Thermal Interface Materials. *Solid State Commun.* **2012**, *152*, 1331–1340.
- (5) Chung, D. D. L. Materials for Thermal Conduction. *Appl. Therm. Eng.* **2001**, *21*, 1593–1605.
- (6) Gao, Y.; Liu, J. Gallium-Based Thermal Interface Material with High Compliance and Wettability. *Appl. Phys. A: Mater. Sci. Process.* **2012**, *107*, 701–708.
- (7) Prasher, R. S.; Koning, P.; Shipley, J.; Devpura, A. Dependence of Thermal Conductivity and Mechanical Rigidity of Particle-Laden Polymeric Thermal Interface Material on Particle Volume Fraction. *J. Electron. Packag.* **2003**, *125*, 386–391.
- (8) Oyharcabal, M.; Olinga, T.; Foulc, M. P.; Vigneras, V. Polyaniline/Clay as Nanostructured Conductive Filler for Electrically Conductive Epoxy Composites. *Synth. Met.* **2012**, *162*, S55–S62.
- (9) Wong, C. P.; Bollampally, R. S. Thermal Conductivity, Elastic Modulus, and Coefficient of Thermal Expansion of Polymer Composites Filled with Ceramic Particles for Electronic Packaging. *J. Appl. Polym. Sci.* **1999**, *74*, 3396–3403.
- (10) Chan, K. L.; Mariatti, M.; Lockman, Z.; Sim, L. C. Effects of the Size and Filler Loading on the Properties of Copper- and Silver-Nanoparticle-Filled Epoxy Composites. *J. Appl. Polym. Sci.* **2011**, *121*, 3145–3152.
- (11) Untereker, D.; Lyu, S.; Schley, J.; Martinez, G.; Lohstreter, L. Maximum Conductivity of Packed Nanoparticles and Their Polymer Composites. *ACS Appl. Mater. Interfaces* **2009**, *1*, 97–101.
- (12) Yu, S. Z.; Hing, P.; Hu, X. Thermal Conductivity of Polystyrene-Aluminum Nitride Composite. *Composites, Part A* **2002**, *33*, 289–292.
- (13) Chung, D. D. L. Carbon Materials for Structural Self-Sensing, Electromagnetic Shielding and Thermal Interfacing. *Carbon* **2012**, *50*, 3342–3353.
- (14) Cai, W.; Moore, A. L.; Zhu, Y.; Li, X.; Chen, S.; Shi, L.; Ruoff, R. S. Thermal Transport in Suspended and Supported Monolayer

Graphene Grown by Chemical Vapor Deposition. *Nano Lett.* **2010**, *10*, 1645–1651.

(15) Hu, L. J.; Liu, J.; Liu, Z.; Qiu, C. Y.; Zhou, H. Q.; Sun, L. F. Thermal Properties of Single-Walled Carbon Nanotube Crystal. *Chin. Phys. B* **2011**, *20*, 096101.

(16) Pettes, M. T.; Ji, H.; Ruoff, R. S.; Shi, L. Thermal Transport in Three-Dimensional Foam Architectures of Few-Layer Graphene and Ultrathin Graphite. *Nano Lett.* **2012**, *12*, 2959–2964.

(17) Li, H.; Srivastava, N.; Mao, J. F.; Yin, W. Y.; Banerjee, K. Carbon Nanotube Vias: Does Ballistic Electron-Phonon Transport Imply Improved Performance and Reliability? *IEEE Trans. Electron Devices* **2011**, *58*, 2689–2701.

(18) Huang, X. Y.; Iizuka, T.; Jiang, P. K.; Ohki, Y.; Tanaka, T. Role of Interface on the Thermal Conductivity of Highly Filled Dielectric Epoxy/AlN Composites. *J. Phys. Chem. C* **2012**, *116*, 13629–13639.

(19) Luo, T. F.; Lloyd, J. R. Enhancement of Thermal Energy Transport Across Graphene/Graphite and Polymer Interfaces: A Molecular Dynamics Study. *Adv. Funct. Mater.* **2012**, *22*, 2495–2502.

(20) Wu, H. P.; Liu, J. F.; Wu, X. J.; Ge, M. Y.; Wang, Y. W.; Zhang, G. Q.; Jiang, J. Z. High Conductivity of Isotropic Conductive Adhesives Filled with Silver Nanowires. *Int. J. Adhes. Adhes.* **2006**, *26*, 617–621.

(21) Pashayi, K.; Fard, H. R.; Lai, F.; Iruvanti, S.; Plawsky, J.; Borca-Tasciuc, T. High Thermal Conductivity Epoxy-Silver Composites Based on Self-Constructed Nanostructured Metallic Networks. *J. Appl. Phys.* **2012**, *111*, 104310.

(22) Burda, C.; Chen, X. B.; Narayanan, R.; El-Sayed, M. A. Chemistry and Properties of Nanocrystals of Different Shapes. *Chem. Rev.* **2005**, *105*, 1025–1102.

(23) Tao, Y.; Yang, Z. G.; Lu, X. L.; Tao, G. L.; Xia, Y. P.; Wu, H. P. Influence of Filler Morphology on Percolation Threshold of Isotropic Conductive Adhesives (ICA). *Sci. China Technol. Sci.* **2012**, *55*, 28–33.

(24) Munari, A.; Xu, J.; Dalton, E.; Mathewson, A.; Razeeb, K. M. Metal nanowire–polymer nanocomposite as thermal interface material. In *59th Electronic Components and Technology Conference U.S.A.*; San Diego, CA, May 26–29, 2009; IEEE: Piscataway, NJ, 2009; Vol. 1–4, pp448–452.

(25) Xu, J.; Munari, A.; Dalton, E.; Mathewson, A.; Razeeb, K. M. Silver Nanowire Array-Polymer Composite as Thermal Interface Material. *J. Appl. Phys.* **2009**, *106*, 124310.

(26) Agyenim, F.; Hewitt, N. The Development of a Finned Phase Change Material (PCM) Storage System to Take Advantage of Off-Peak Electricity Tariff for Improvement in Cost of Heat Pump Operation. *Energy Build.* **2010**, *42*, 1552–1560.

(27) Wu, H.; Hu, L.; Rowell, M. W.; Kong, D.; Cha, J. J.; McDonough, J. R.; Zhu, J.; Yang, Y.; McGehee, M. D.; Cui, Y. Electrospun Metal Nanofiber Webs as High-Performance Transparent Electrode. *Nano Lett.* **2010**, *10*, 4242–4248.

(28) Alouach, H.; Mankey, G. J. Texture Orientation of Glancing Angle Deposited Copper Nanowire Arrays. *J. Vac. Sci. Technol. A* **2004**, *22*, 1379–1382.

(29) Kudo, H.; Fujihira, M. DNA-Templated Copper Nanowire Fabrication by a Two-Step Process Involving Electroless Metallization. *IEEE Trans. Nanotechnol.* **2006**, *5*, 90–92.

(30) Lisiecki, I.; Pileni, M. P. Synthesis of Well-Defined and Low Size Distribution Cobalt Nanocrystals: The Limited Influence of Reverse Micelles. *Langmuir* **2003**, *19*, 9486–9489.

(31) Mohl, M.; Pusztai, P.; Kukovecz, A.; Konya, Z.; Kukkola, J.; Kordas, K.; Vajtai, R.; Ajayan, P. M. Low-Temperature Large-Scale Synthesis and Electrical Testing of Ultralong Copper Nanowires. *Langmuir* **2010**, *26*, 16496–16502.

(32) Rathmell, A. R.; Wiley, B. J. The Synthesis and Coating of Long, Thin Copper Nanowires to Make Flexible, Transparent Conducting Films on Plastic Substrates. *Adv. Mater.* **2011**, *23*, 4798–4803.

(33) Jin, M.; He, G.; Zhang, H.; Zeng, J.; Xie, Z.; Xia, Y. Shape-Controlled Synthesis of Copper Nanocrystals in an Aqueous Solution with Glucose as a Reducing Agent and Hexadecylamine as a Capping Agent. *Angew. Chem., Int. Ed.* **2011**, *50*, 1–6.

(34) Kevin, M.; Ong, W. L.; Lee, G. H.; Ho, G. W. Formation of Hybrid Structures: Copper Oxide Nanocrystals Templated on Ultralong Copper Nanowires for Open Network Sensing at Room Temperature. *Nanotechnology* **2011**, *22*, 235701.

(35) Zhang, D.; Wang, R.; Wen, M.; Weng, D.; Cui, X.; Sun, J.; Li, H.; Lu, Y. Synthesis of Ultralong Copper Nanowires for High-Performance Transparent Electrodes. *J. Am. Chem. Soc.* **2012**, *134*, 14283–14286.

(36) Baumgard, J.; Vogt, A. M.; Kragl, U.; Jähnisch, K.; Steinfeldt, N. Application of Microstructured Devices for Continuous Synthesis of Tailored Platinum Nanoparticles. *Chem. Eng. J.* **2013**, *227*, 137–144.

(37) Yu, H.; Li, L.; Zhang, Y. Silver Nanoparticle-Based Thermal Interface Materials with Ultra-Low Thermal Resistance for Power Electronics Applications. *Scr. Mater.* **2012**, *66*, 931–934.

(38) Gao, L.; Zhou, X. F.; Ding, Y. L. Effective Thermal and Electrical Conductivity of Carbon Nanotube Composites. *Chem. Phys. Lett.* **2007**, *434*, 297–300.

(39) Yu, S.; Lee, J.-W.; Han, T. H.; Park, C.; Kwon, Y.; Hong, S. M.; Koo, C. M. Copper Shell Networks in Polymer Composites for Efficient Thermal Conduction. *ACS Appl. Mater. Interfaces* **2013**, *5*, 11618–11622.

(40) Shahil, K. M.; Balandin, A. A. Graphene-Multilayer Graphene Nanocomposites as Highly Efficient Thermal Interface Materials. *Nano Lett.* **2012**, *12*, 861–867.

(41) Debelak, B.; Lafdi, K. Use of Exfoliated Graphite Filler to Enhance Polymer Physical Properties. *Carbon* **2007**, *45*, 1727–1734.

(42) Bryning, M. B.; Milkie, D. E.; Islam, M. F.; Kikkawa, J. M.; Yodh, A. G. Thermal Conductivity and Interfacial Resistance in Single-Wall Carbon Nanotube Epoxy Composites. *Appl. Phys. Lett.* **2005**, *87*, 161909.

(43) Liu, C. H.; Huang, H.; Wu, Y.; Fan, S. S. Thermal Conductivity Improvement of Silicone Elastomer with Carbon Nanotube Loading. *Appl. Phys. Lett.* **2004**, *84*, 4248–4250.

(44) Harada, M.; Hamaura, N.; Ochi, M.; Agari, Y. Thermal Conductivity of Liquid Crystalline Epoxy/BN Filler Composites Having Ordered Network Structure. *Composites, Part B* **2013**, *55*, 306–313.

(45) Zhou, Y.; Wang, L.; Zhang, H.; Bai, Y.; Niu, Y.; Wang, H. Enhanced High Thermal Conductivity and Low Permittivity of Polyimide Based Composites by Core-Shell Ag@SiO<sub>2</sub> Nanoparticle Fillers. *Appl. Phys. Lett.* **2012**, *101*, 012903.

(46) Hands, D.; Lane, K.; Sheldon, R. P. Thermal Conductivities of Amorphous Polymers. *J. Polym. Sci., Part C* **1973**, *42*, 4717–4726.

(47) Luan, V. H.; Tien, H. N.; Cuong, T. V.; Kong, B. S.; Chung, J. S.; Kim, E. J.; Hur, S. H. Novel Conductive Epoxy Composites Composed of 2-D Chemically Reduced Graphene and 1-D Silver Nanowire Hybrid Fillers. *J. Mater. Chem.* **2012**, *22*, 8649–8653.